Phase Transitions and Annealing Temperature Effect on Thermoelectric Properties of Zinc–Antimony Thin Films

Ahmed Radhi Salim[1], Hisham Mohammed Ali Hasan[2]

[1]Physics Department College of Education; University of Al-Qadisiyah, Diwaniyah, Iraq,
Email: Phy.post22@qu.edu.iq
[2]Physics Department College of Education; University of Al-Qadisiyah, Diwaniyah, Iraq,
Email: hisham.hasan@qu.edu.iq

ABSTRACT
ZnSb samples were prepared by cold pressing technique for bulk and co-sputtering for thin film, followed by 337k, annealing temperature. The structural and morphological analysis of the samples has been carried out by X-ray diffraction (XRD), and Scanning electron microscope (SEM) techniques. XRD analysis confirms the orthorhombic ZnSb phase, orthorhombic crystal structure with different space groupsfor Zn_8Sb_7 thin film,and $Zn_{36}Sb_{30}$ with crystal system of trigonal for annealing thin film samples. The figures of meritand Seebeck coefficientvalues of zinc antimony samples were measured. The experimental results demonstrated zinc antimony with differentcrystal structures is a promising approach to enhancing the thermoelectric properties of ZnSb.The electric properties, Hall effect, and carrier concentrations of ZnSb during phase transitions were studied to optimize its performance.

Keywords: zinc antimony, thin film, thermoelectric properties.

1. INTRODUCTION

Many technological applications require thermoelectric (TE) materials as they can directly transform heat energy into electrical energy and vice versa through the Seebeck and Peltier effects. Here are some key points highlighting their importance, the value of thermoelectric materials lies in their capacity to harness waste heat, provide sustainable power generation solutions, facilitate thermal management in diverse environments, and help develop energy-efficient technologies in various industries [1,2].

Zinc-antimony (ZnSb)system affords a semiconductor phase with a covalent framework structure containing multicenter bonded structural entities and has been known as thermoelectric materials, the diverse crystal structures of zinc antimony compounds are responsible for lattice thermal conductivity, which is attributed to the presence of various forms of disorder and large-sized unit cells [3]. Thermoelectric (TE) devices using thin films have attracted much interest because they can act as self-powered sources that can harness electricity from temperature differences between electronic components and their surroundings,this technology holds the promise of compact and convenient power generation [4,5]. Therefore, there is an urgent requirement to develop high-performance thin films that are not only cost-effective but also environmentally friendly and free of toxic substances. This practice has become central to the field of thermoelectricity [6]. The dimensionless figure of merit zT is used to assess the effectiveness of TE materials, and provide a TE device with a decent efficiency, TE materials with zT> 1 are usually needed[7]. However, for commercial applications, it's also crucial that the TE material be composed of inexpensive, readily available elements using an economical synthesis technique [8]. The exploration of thin films opens up a wide array of potential applications beyond traditional bulk materials, especially in the realm of low-power devices and microsystems[9]. With benefits including improved surface qualities, lower material consumption, and compatibility with microfabrication methods, thin films are very appealing for a wide range of applications,thin films offer several advantages such as miniaturization, flexibility, and the ability to tailor material properties at the nanoscale, making them well-suited for applications where low power consumption and small form factors are critical. Zinc antimonide ZnSb thin films are sensitive to a variety of parameters, including temperature, pressure, and gas composition, their characteristics may be tailored for certain sensor applications[10,11].

The stability of the many known phases has been closely examined, and the Zn-Sb binary phase diagram has garnered a lot of interest. The physical characteristics and stability of a recently detected Zn_8Sb_7 phase have been estimated by theoretical calculations based on experimental data. ZnSb films and two entirely novel meta-stable crystalline phases of zinc antimonide were directly formed on silica substrates

using a co-sputtering technique in the current work. The identification of novel zinc antimonide phases. It is interesting to learn about the stability and attributes of the Zn_8Sb_7 phase by theoretical calculations after it was identifiedexperimentally[12,13,14].A noteworthy accomplishment is the ability to use a co-sputtering technique to directly deposit ZnSb films and identify novel meta-stable crystalline phases of zinc antimonide on silica substrates, Overall, this research contributes to a deeper understanding of the Zn-Sb binary system and opens up possibilities for further exploration of its phase diagram and material properties.

2. Material and Thin Film Synthesis

High-purity Sb (99.99%) and Zn (99.99%) targets were deposited in a sputtering chamber. The target-substrate distance was fixed at 10 cm, and both sputtering angles were adjusted to 45°. The pressure within the chamber was reduced to 6 104 Pa while maintaining a 30 sccm flow rate of the sputtering gas Ar. After that, the operating pressure was raised to 0.5 Pa. After the Sb precursor layer was first placed, glass substrates were ultrasonically cleaned in acetone and alcohol for sixty minutes before being used. The same deposition method was used to create zinc layers on top of the antimony precursor layers, but a fixed sputtering power of 25 W was used. The thickness of ZnSb layers of377 nm, with the use of a scanning electron microscope (SEM, SUPRA 55), the surface morphologies were measured. With a CuKα radiation of 0.15406 nm, the phase compositions of bulk and thin film crystallographic structures were characterized by X-ray diffraction (XRD, Ultima IV, Rigaku, Tokyo, Japan) in the traditional 2θ mode range of 20°–80°. Using the Seebeck coefficient measuring equipment (SBA-458) in a helium environment, the electrical conductivity and Seebeck coefficient of the thin films were measured at temperature ranges of 300 to 673 K. The Seebeckcoefficient and the figure of merit are measured at variousannealing temperatures. Hall effect and charge carrier concentration measured for zinc antimonide samples.

3. RESULT AND DISCUSSION

The structural, electrical, and phase transitions of ZnSb bulk and thin film were described here. Fig. 1 Exhibits XRD profiles for the bulk ZnSband thin film synthesis before and after being annealed withthermal evaporationof377 nm thickness. Fig 1 (a) shows XRD patterns of bulk zinc antimony ZnSband compares it to the standard diffraction data (JCPDS: 89-2998),which is indexed based on bulk orthorhombic ZnSb with space group P b c a (61) and cellparameters (a= 6.2180 A^0, b= 7.7410 A^0, c= 8.1150 A^0). The peaks (112),(121) and (211) dominate the whole PXRD pattern respectively. As-deposited a Zn_8Sb_7thin film is almost amorphous with some reflections from Zn_8Sb_7 (Fig. 1b),Rietveld refinement using the model with phaseof β-Zn_8Sb_7indexed orthorhombic crystal structure, P m n 21 (31) space group and with cell parameters (a=15.0291 A^0, b= 7.7310 A^0, c=12.7431 A^0), ICSD No. 238947, the peaks (213), (411), and (622) are dominating the whole pattern. With 10 Sb_2^{4-} dimers and 8 isolated Sb^{3-} anions, There are twenty-four Zn atoms distributed over six fully occupied crystallographic sites (Zn1–Zn6) and the other 8 Zn atoms are distributed over 4 partially occupied sites (Zn7, Zn8, Zn9 and Zn10) as shown in Figure 2 [15,16].

Fig 1. XRD patterns ZnSb: (a) bulk powder, and (b), (c) ZnSb thin film before and after being annealed respectively.
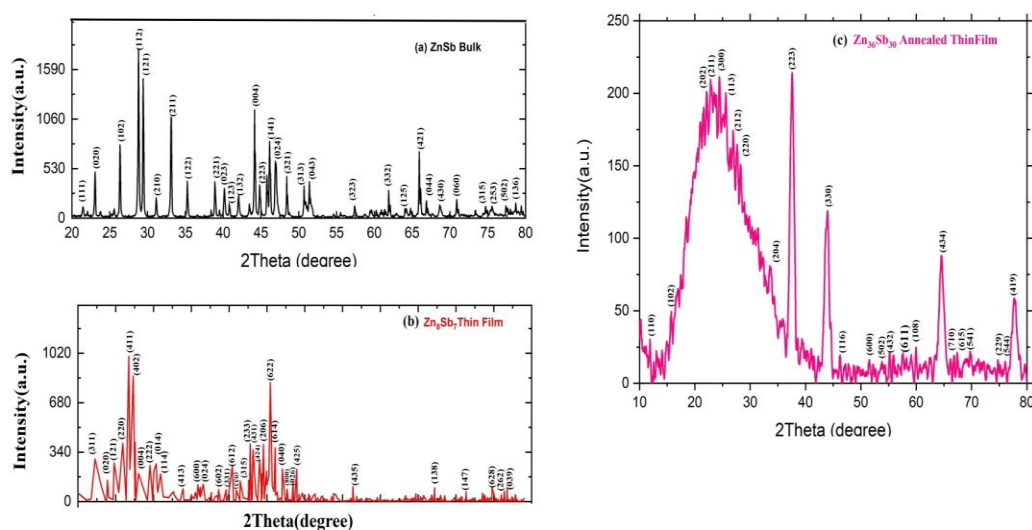
An annealing treatment under Ar atmosphere at 377 K for 2 h results in a phase transition of Zn_8Sb_7 thin film into $Zn_{36}Sb_{30}$($(Zn_4 Sb_3)_{3.14}$)as evident from the PXRD pattern shown in Figure 1 c, where all the PXRD peaks of the annealed sample can be assigned to $Zn_{36}Sb_{30}$ with crystal system of trigonal (hexagonal axes), space group R -3 c and of cellparameters, a = 12.2310 A^0, c = 12.4170 A^0. , The peaks (300), (223), (330),(434) and (419) are dominating the whole pattern(standardcard no [00-006-0208]), the XRD pattern showsthe semicrystalline pattern at low angels, and it starts to crystallize in a metastable phase, the entire film may not undergo a complete transformation into a fully crystalline phase due to the annealing process, resulting in distinct peaks from the crystalline regions and a broad background contribution from the amorphous regions, resulting in a semicrystalline pattern.
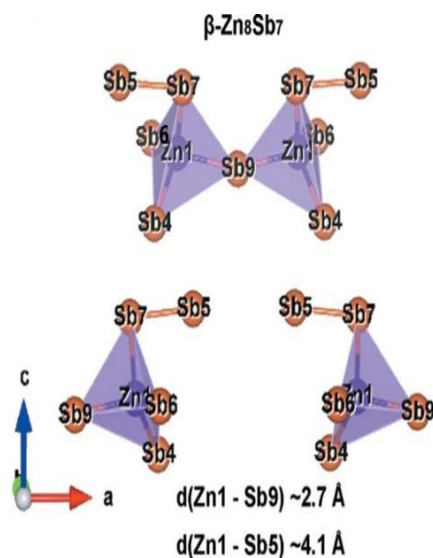
Fig 2. Zn1-centered tetrahedra for the β-Zn8Sb7 phase [16].

The complex interplay between kinetics, thermodynamics, chemical bonding, and material defects causesZnSb to show a wide variety of crystalline morphologies. Three distinct crystalline forms exist for zinc sulphide: the orthorhombic structure, which is the most common and stable phase at normal temperature, the hexagonal structure, which may form at high temperatures and be rapidly quenched, and the trigonal crystal system[17,18]. In addition, the temperature-dependent electrical resistivity (ρ) and Seebeck coefficient (S) were measured for bulk ZnSb, thin film $Zn_{36}Sb_{30}$, and annealed thin film which shows the β-Zn_8Sb_7 phase,Figure 3 and Table 1. ,display Seebeck coefficients were positive over the whole temperature range, suggesting that holes are important charge carriers in p-type semiconductors.
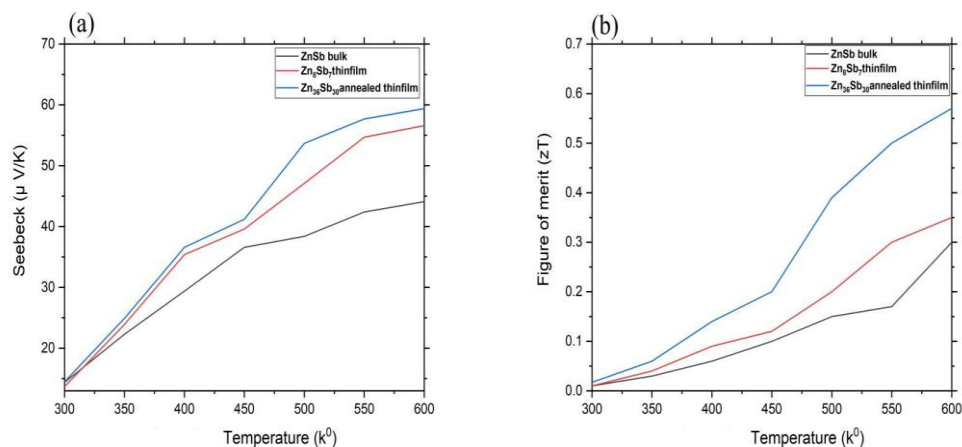
Fig 3. (a) Seebeck value for ZnSb samples changes with temperature. (b) a figure of merit(ZT) values for ZnSb samples changes with temperature.

Table 1. Seeback and figure of merit for ZnSb materials.

	ZnSb bulk		Zn_8Sb_7 thin film		$Zn_{36}Sb_{30}$ annealed thin film	
Temperature	Seebeck(µ V/K)	Figure of merit (ZT)	Seebeck (µ V/K)	Figure of merit (ZT)	Seebeck(µ V/K)	Figure of merit (ZT)
300 (k^0)	13.7	0.01	14.45	0.01	14.5	0.017
350 (k^0)	22.3	0.03	23.9	0.036	24.9	0.06
400 (k^0)	29.4	0.06	35.4	0.09	36.6	0.14
450 (k^0)	36.6	0.11	39.6	0.13	41.2	0.2
500 (k^0)	38.4	0.134	47.1	0.2	53.7	0.39
550 (k^0)	42.4	0.18	54.8	0.3	57.7	0.5
600 (k^0)	44.1	0.21	56.6	0.35	59.4	0.57

As the material undergoes a quantum confinement transition from bulk to thin film, the density of states changes, enhancing the Seebeck coefficient and decreasing thermal conductivity. These changes also cause the Seebeck and figure of merit values to increase with rising temperature. The thermal conductivity includes both the lattice and electronic contributions, in thin films, have often lower values due to increasing boundary scattering of phonons,the difference between bulkZnSb orthorhombic space group P b c (61) and thin film Zn_8Sb_7 orthorhombic space group P m n (21), while both structures are orthorhombic, the exact positioning and environment of atoms will vary based on the specific space group, then the two space groups have different Zn sets of symmetry operations, which means that the atomic arrangements and the resulting physical properties of the material can differ significantly[19].

The thermoelectric properties of ZnSb can vary significantly depending on its crystal structure, XRD pattern (Figure 1) illustrated bulk ZnSb with orthorhombic space group Pbc(61), ZnSb thin film with orthorhombic space group Pmn(21) and ZnSb annealed thin film trigonal (hexagonal axes) with space group R -3 c space group. Orthorhombic structures can have anisotropic electrical conductivity due to the directional dependence of their atomic arrangements, and low thermal conductivity can be expected in materials with complex atomic arrangements due to increased phonon scattering of orthorhombic structure with space group Pmn(21). different atomic arrangement and symmetry operations can lead to variations in conductivity. Orthorhombic crystal structures with space groupsPbc(61) and Pmn(21) have different atomic arrangements leading to different electronic band structures arising from the distinct atomic positioning and variations in phonon scattering mechanisms. Trigonal structures in space group R -3 c often have more isotropic properties compared to orthorhombic structures. Electrical conductivity may be higher due to more symmetric atomic arrangements, and then the Seebeck coefficient in trigonal structures might be more uniform and can potentially be optimized for thermoelectric applications[20].

Table 2. The electrical properties of zinc antimony ZnSb samples were obtained by Hall effect measurement.

Samples	ZnSb bulk	Zn_8Sb_7 thin film	$Zn_{36}Sb_{30}$ annealed thin film at 350 k^0
Hall coefficient (m^3/coulomb)	97×10^3	15×10^3	25×10^3
Carrier concentration (m^{-3})	0.64×10^{14}	4.114×10^{14}	2.51×10^{14}

ZnSb samples' electrical characteristics were assessed using the Hall effect method at room temperature and 350 k^0. A positive Hall coefficient is seen in Table 2,depending on the phase shifts that annealing causes in the material's characteristics, the Hall coefficient is a material-specific metric that might be affected. Positively charged holes dominate the material's charge carrier distribution when the Hall coefficient is positive. This is characteristic of p-type semiconductors, in which the valence band's lack of electrons, or holes, serves as the charge carrier. Increased phonon, impurity, or defect scattering can cause a material's charge carrier mobility to decrease, which in turn can alter the Hall coefficient. The carrier concentration and mobility are closely related to the Hall coefficient. The intricate interaction between material qualities and environmental variables may be seen in the considerable changes in the Hall coefficient value caused by increased scattering, which decreases mobility.

Figures 4(a), 4(b), and 4(c) demonstrate that the as-grown thin film is beginning to crystallize in a metastable phase while remaining amorphous.
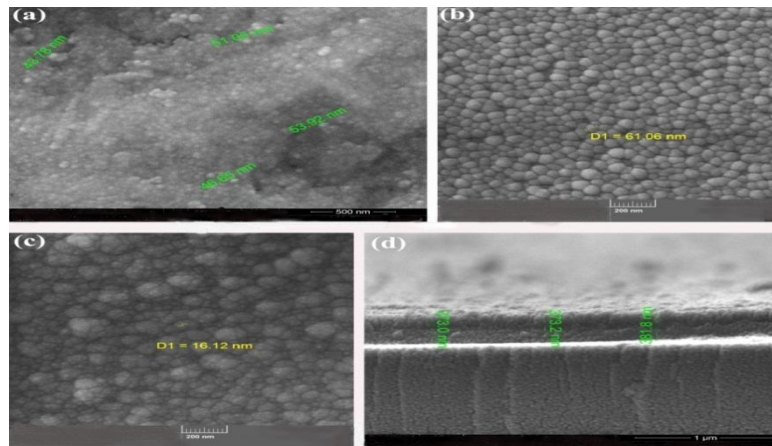
Fig.4 (a)SEM images of ZnSb nanoparticles bulk sample. (b) Image of a Zn_8Sb_7 thin film nanoparticle (c) SEM image sample of $Zn_{36}Sb_{30}$ annealed thin film. (d) Thickness measurement result for film thicknesses.

Figure 1(b) demonstrates unequivocally that during the early stages of the transition from the amorphous phase to the metastable phase, the peak intensities of the metastable phase increase with rising temperature, suggesting that the amount of amorphous constituent decreases as temperature rises.

The grain sizes are approximations and can vary based on crystal structure annealing temperature, and precursor concentration. The grains observed in the SEM images are on the nanometer scale. This suggests that the film is composed of small, discrete crystallites rather than large, continuous crystals. Although all samples exhibit a porous morphology, slight differences are observed between them. These differences might be attributed to variations in the deposition process or slight changes in annealing conditions, where thermal treatment provides energy for atoms to migrate and rearrange, leading to grain growth. The increase in grain size with annealing could affect the electrical and thermal properties of the ZnSb thin films. For instance, larger grains might reduce grain boundary scattering, potentially improving electrical conductivity.

4. CONCLUSION

Several zinc antimonide ZnSb bulk samples with orthorhombic crystal structures and thin films deposited by co-sputerring method, based on the microstructure results, the prepared zinc antimonide thin film have Zn_8Sb_7 orthorhombic crystal structures with different space group from the bulk, after annealing and transforms to another crystal structure $Zn_{36}Sb_{30}$ crystal structure,Our first principles investigation has shown that the phase transition of zinc antimonide by results in p-type compounds with a maximum figure of merit of 0.57 at 600K for $Zn_{36}Sb_{30}$ crystal structure. The Zn_8Sb_7 thin film exhibits the highest positive hole carrier concentration, which is significant for its electrical conductivity.

Declarations
More concise: "A comprehensive range of concerns should be considered and reported."

Conflict of Interest
The authors declare that they have no competing interests.

Ethical Approval
This research adhered to the ethical principles outlined in the Declaration of Helsinki. The study was approved by the Ethics Committee of the Physics Department at Al-Qadisiyah University, College of Education.

Informed Consent
The local ethics committee reviewed the research methodology, participant details, and informed consent form.

REFERENCES

[1] G.Y.Senguler et al.,2023,"Effect of sulfur concentration on structural, optical and electrical properties of Cu_2CoSnS_4 absorber film for photovoltaic devices",Phys. B: Condens. Matter, 648, 414424,doi.org/10.1016/j.physb.2022.414424

[2] I.M. El Radaf et al.,2021,"Structural and optical characterizations of the thermally evaporated $Pb_xGa_{1-x}Se$ thin films", Optik, 238,166610, DOI:10.1016/j.ijleo.2021.166610

[3] A.A. Faremi et al.,2022,"Scalability of copper selenide (CuSe) thin films using electrodeposition technique with three electrode configurations for solar energy applications", Materials Letters,314(5):131868, DOI: 10.1016/j.matlet.2022.131868

[4] A.Parida et al.,2022,"Impact on nonlinear/linear optical and structural parameters in quaternary $In_{15}Ag_{10}S_{15}Se_{60}$ thin films upon annealing at different temperatures,Ceram. Int., 48, 11, PP. 15380-15389, https://doi.org/10.1016/j.ceramint.2022.02.072.

[5] I.M. El Radaf et al.,2022,"Highlights on the structural, optical, and optoelectrical properties of novel $InSbO_3$ thin films synthesized by chemical bath deposition,"J. Non-Cryst. Solids,588,121612,doi.org/10.1016/j.jnoncrysol.2022.121612.

[6] J. Sun et al.,2022,"Study on piezo-phototronic effect of AlZnO thin film flexible ultraviolet photodetector", Phys. E Low. Dimens. Syst. Nanostruct., 140, 115149, doi.org/10.1016/j.physe.2022.115149.

[7] J. R. Sootsman , D. Y. Chung , M. G. Kanatzidis "New and old concepts in thermoelectric materials" , Angew. Chem. Int.Ed., 48, 8616 ,DOI: 10.1002/anie.200900598

[8] B. B. Iversen , 2010,"Fulfilling thermoelectric promises: β-Zn_4Sb_3 from materials research to power generation ",J. Mater. Chem. 2010,**20**, 10778

[9] X. F. Qiu , L. N. Austin , P. A. Muscarella , J. S. Dyck , C. Burda , 2006,"Nanostructured Bi2Se3 Films and Their Thermoelectric Transport Properties",Angew.Chem. Int. Ed., 45, 5656 ,doi.org/10.1002/anie.200600848.

[10] M. Takashiri , K. Miyazaki , S. Tanaka , J. Kurosaki , D. Nagai ,H. Tsukamoto , 2008," Effect of grain size on thermoelectric properties of -type nanocrystalline bismuth-telluride based thin films J. Appl. Phys., 104, 084302 ,doi.org/10.1063/1.2990774.

[11] Jian Wang,Kirill Kovnir,2015,"Elusive β-Zn_8Sb_7: A New Zinc Antimonide Thermoelectric",J. Am. Chem. Soc.2015, 137, 39, 12474–12477,doi.org/10.1021/jacs.5b08214.

[12] Lirong Song, Martin Roelsgaard, Anders B. Blichfeld,and et.al.,2021," Structural evolution in thermoelectric zinc antimonide thin films studied by in situ X-ray scattering techniques", MATERIALS | COMPUTATION,IUCrJ, 8,Part 3,PP. 444-554,doi.org/10.1107/S2052252521002852.

[13] D. Sidharth,Bhuvanesh Srinivasan,A.S. AlagarNedunchezhian,and et.al,2022,"Enhancing the thermoelectric performance of nanostructured ZnSb by heterovalent bismuth substitution**,**Journal of Physics and Chemistry of Solids**,**Volume 160, 110303, https://doi.org/10.1016/j.jpcs.2021.110303.

[14] JothilalPalraj, Muhammad Sajjad, Manojkumar Moorthy, and et al.,2024," High thermoelectric performance in p-type ZnSb upon increasing Zn vacancies: an experimental and theoretical study", J. Mater. Chem. **A**, Advance Article,doi.org/10.1039/D4TA01659A

[15] Jian Wang, Kirill Kovnir,2015,"Elusive β-Zn_8Sb_7: A new zinc antimonide thermoelectric",Journal of the American Chemical Society, 137,39,DOI: 10.1021/jacs.5b08214.

[16] Lirong Song, Martin Roelsgaard, Anders B. Blichfeld,and et.al.,2021," Structural evolution in thermoelectric zinc antimonide thin films studied by in situ X-ray scattering techniques", IUCrJ , 8, PP.444–454, https://doi.org/10.1107/S2052252521002852

[17] Ignat'ev, N.A.; Ugai, Ya.A.; Aleinikova, K.B.; Rabotkina, N.S.,1971," Structure of beta-Zn_4 Sb_3 and Cd_4 Sb_3", Journal of Structural Chemistry (USSR) (ZhurnalStrukturnoiKhimii), 1971, 12, PP.665-666.

[18] ProtimaRauwel, Ole Martin Løvvik, ErwanRauwel, and et. al,2011,"Nanostructuring in b-Zn4Sb3 with variable starting Zn compositions",Phys. Status Solidi A 208, No. 7, PP. 1652–1657 , DOI 10.1002/pssa.201026613.

[19] Mohsen K. Keshavarz, Chun-Wan Timothy Lo, Sylvain Turenne. and et. al.,2019,"Hot Extrusion of ZnSb-Based Thermoelectric Materials; A Novel Approach for Scale-Up Production",J. Manuf. Mater. Process. 2, 3, 58; doi:10.3390/jmmp3030058

[20] R. Biswas , S. Mukherjee , R.C. Mallik , S. Vitta , T. Dasgupta,2019," Ultralow thermal conductivity and low charge carrier scattering potential in Zn1-xCdxSb solid solutions for thermoelectric application", Materials Today Energy, 12, PP. 107-113,https://doi.org/10.1016/j.mtener.2018.12.014.